Supporting Information

Title: The cornucopia of structures in the pseudobinary system (SnSe)xBi2Se3 – A crystal-chemical copycat

Authors: *Frank Heinke,[a] Philipp Urban,[a] Anton Werwein,[a] Christina Fraunhofer,[a,b] Tobias Rosenthal,[b] Stefan Schwarzmüller,[a] Daniel Souchay,[a] Felix Fahrnbauer,[a] Vadim Dyadkin,[c] Gerald Wagner[a] and Oliver Oeckler[a,]***

a) Leipzig University, Faculty of Chemistry and Mineralogy, IMKM, Scharnhorststr. 20, 04275 Leipzig, Germany
b) LMU Munich, Department of Chemistry, Butenandtstr. 5-13 (D), 81377 Munich, Germany
c) European Synchrotron Radiation Facility, 71 avenue des Martyrs, CS 40220, 38043 Grenoble, France

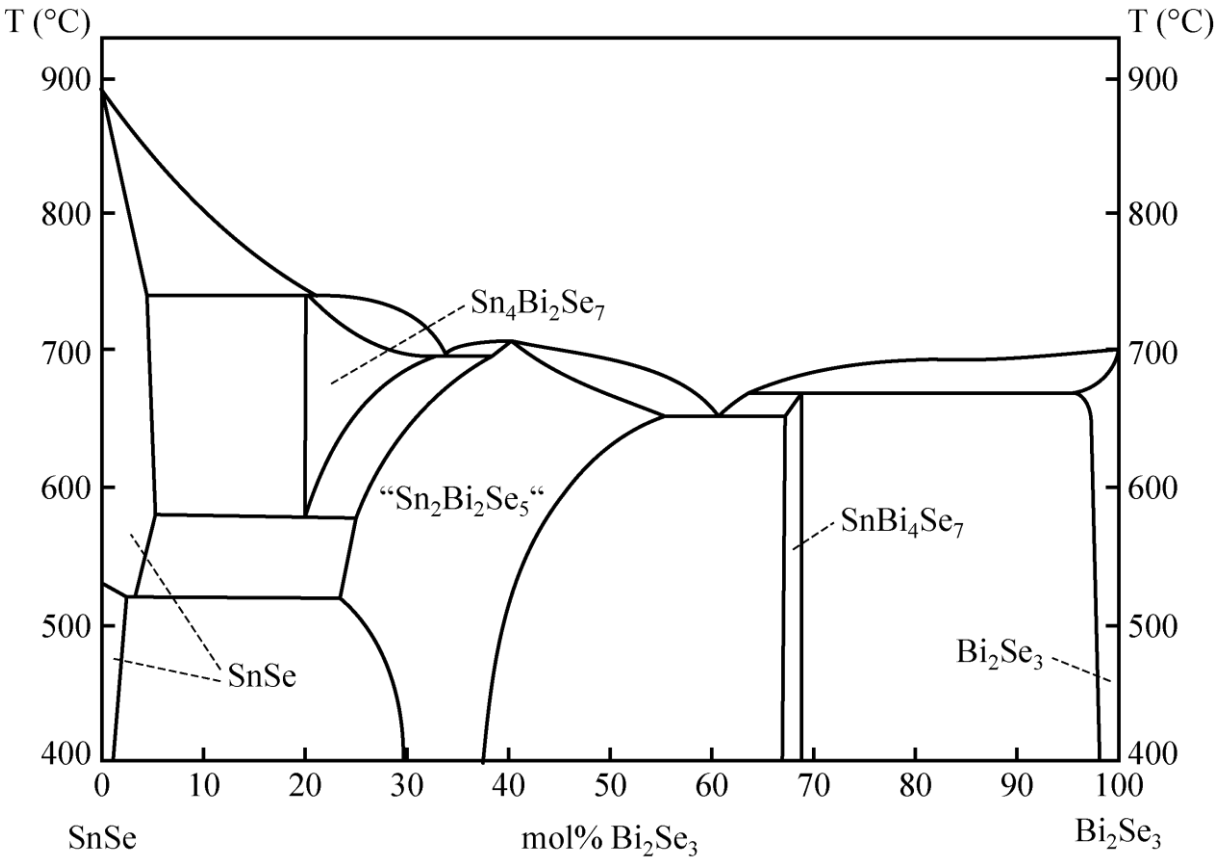

Figure S1: Phase diagram for the pseudo-binary system SnSe-Bi_2Se_3, redrawn from: Adouby, K.; Elidrissi Moubtassim, M. L.; Vicente, C. P.; Jumas, J. C.; Touré, A. A. X-ray diffraction, ^{119}Sn Mössbauer and thermal study of SnSe–Bi_2Se_3 system. *J. Alloys Compd.* **2008**, *453*, 161-166.

Table S1: Synthesis parameters of ternary tin bismuth selenides: nominal compositions, local sample names, melting conditions, annealing conditions (including remarks on quenching to room temperature) and parameters for chemical transport reaction as well as information on the utilization of the respective samples.

nominal composition **sample name**	**used for …**	**melting at …** **- quenched in …**	**annealing at …** **- then quenched in …**	**chemical transport** **temperature (hot/cold)**	**chemical transport** **transport agent**
$(SnSe)_3Bi_2Se_3$ PUT062	a) PXRD b) SEM-EDX	950 °C (for 21 h) - H_2O	---	---	---
$(SnSe)_4Bi_2Se_3$ ** PUT060	a) PXRD b) SCXRD c) SEM-EDX	940 °C (for 17.5 h) - H_2O	---	640 °C / 585 °C (for 19 h)	3.6 mg I_2
$(SnSe)_4Bi_2Se_3$ *** PUT078	a) thermoelectric characterization b) PXRD	940 °C (for 2.5 h) - air	---	---	---
$(SnSe)_4Bi_2Se_3$ PU086	a) thermoelectric characterization b) PXRD	940 °C (for 4 h) - air	---	---	---
$(SnSe)_5Bi_2Se_3$ * PUT066	a) PXRD	940 °C (for 19.5 h) - N_2 (liquid)	---	---	---
$(SnSe)_{0.5}Bi_2Se_3$ ** PUT069	a) PXRD b) SCXRD c) TEM study	940 °C (for 21.5 h) - H_2O	620 °C (for 167 h) - air	547 °C / 445 °C (for 94 h)	4.6 mg I_2
$(SnSe)_{0.5}Bi_2Se_3$ *** FRHW13	a) thermoelectric characterization b) PXRD c) TEM study	900 °C (for 48.5 h) - air	500 °C (for 167 h) - H_2O	---	---
$(SnSe)_2Bi_2Se_3$ PUT071	a) PXRD b) SCXRD	940 °c (for 3 h) - H_2O	620 °C (163 h) - H_2O	---	---
$(SnSe)_2Bi_2Se_3$ *** FRHW32	a) thermoelectric characterization b) PXRD c) TEM study d) resonant SCXRD measurements	900 °C (for 0.5 h) - slow cooling	620 °C (for 264 h) - H_2O	---	---
$(SnSe)_{\sim 1.86}Bi_2Se_3$ FRHW09	a) PXRD b) resonant SCXRD measurements	900 °C (for 24 h) - H_2O	530 °C (for 120 h) - H_2O	---	---
$(SnSe)_{1.5}Bi_2Se_3$ PU089	a) PXRD b) SCXRD c) SEM-EDX	a) 900 °C (for 72 h) - air b) 900 °C (19) - slow cooling to 550 °C	550 °C (for 90 h) - air	---	---

* For quenching in liquid nitrogen, an ampoule containing the melt was removed from the furnace at 940 °C and cracked open at a predetermined breaking point so that the liquid melt could be poured on an aluminium plate cooled with liquid nitrogen.

** For chemical vapor transport, ~150 mg of fused and air-quenched materials were crushed and sealed in silica glass ampoules (length ~20 cm, diameter 15 mm) under vacuum with ~3 wt% iodine (Alfa Aesar, sublimed, 99.8 %) as transport agent. Chemical vapor transport took place in a two-zone furnace.

*** Samples for the thermoelectric characterization of $(SnSe)_4Bi_2Se_3$, $(SnSe)_{0.5}Bi_2Se_3$ and $(SnSe)_2Bi_2Se_3$ (total weight ~3 g each) were synthesized in a similar way as the melt-quenched or annealed samples of smaller total weight, using ampoules with a flat bottom (length ~10 cm, diameter 15 mm). After removing them from the furnace, they were fixed in vertical orientation in order to solidify the melt as a flat ingot on the bottom of the ampoule. These ingots were polished with SiC grinding powder and cut to cuboid shapes when necessary.

Table S2: Experimental densities of samples for thermoelectric characterization compared with the corresponding theoretical ("X-ray") densities derived from crystal structure data.

chemical composition	structure type	experimental density in g/cm³	theoretical density in g/cm³	percentage of theoretical density
$Sn_4Bi_2Se_7$	NaCl	6.500	6.581 (single crystal data)	98.8 %
$SnBi_4Se_7$	$GeSb_2Te_4$	7.218	7.324	98.6 %
„$Sn_2Bi_2Se_5$"	L4,4 lillianite	6.828	6.854"	99.6 %

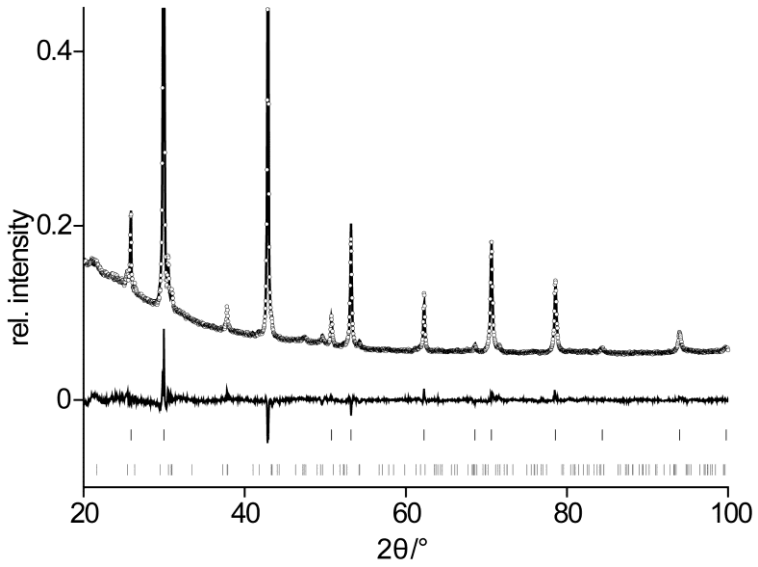

Figure S2: Rietveld refinement for a melt-quenched sample with the nominal composition $Sn_5Bi_2Se_8$ (x = 5, the strongest reflection is truncated at 45% of the maximum intensity): data points are drawn as circles, calculated data as a black line, difference plot as a black line below, reflection positions indicated by vertical lines for the cubic phase (top row) and for SnSe (bottom row).

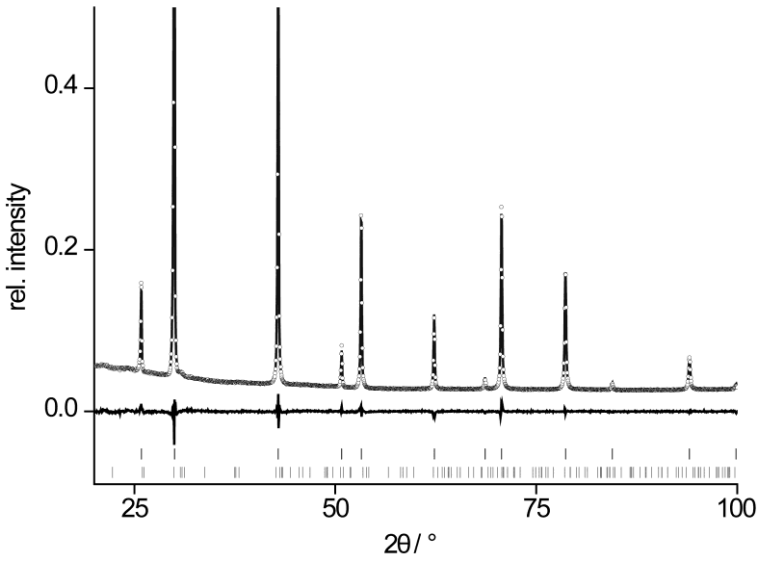

Figure S3: Rietveld refinement for a melt-quenched sample with the composition $Sn_4Bi_2Se_7$ (x = 4, the strongest reflection is truncated at 50% of the maximum intensity): data points are drawn as circles, calculated data as a black line, difference plot as a black line below, reflection positions indicated by vertical lines for the cubic phase (top row) and for SnSe (bottom row).

Table S3: Crystal data and results of the Rietveld refinement of quenched $Sn_5Bi_2Se_8$ = $Sn_{0.625}Bi_{0.25}Se$). Also note the footnote of Table S3.

formula	$Sn_{0.582}Bi_{0.279}Se$ *	SnSe
phase fraction	90 wt-%	10 wt-%
formula mass	205.39 $gmol^{-1}$	197.67 $gmol^{-1}$
crystal system	cubic	orthorhombic
space group	*Fm$\bar{3}$m*	*Pnma*
cell parameters	a = 5.95931(13)Å	a = 11.541(2) Å b = 4.1663(9) Å c = 4.3976(11) Å
cell volume	211.636(2) $Å^3$	211.45(8) $Å^3$
X-ray density	6.4764 (4) gcm^{-3}	6.209(2) gcm^{-3}
Z	4	4
R_{Bragg}	0.036	0.022
radiation	Cu-$K_{\alpha1}$ (λ = 1.54051 Å)	
2θ range	4° < 2θ < 100°	
refined parameters	31, thereof 18 for background	
R_p / R_{wp}	0.016 / 0.023	
GooF	1.148	

* The composition was constrained to $Sn_{0.582}Bi_{0.279}Se$. This takes into account the exsolution of SnSe according to the following reaction equation: $Sn_{0.625}Bi_{0.25}Se$ → 0.104 SnSe + $Sn_{0.521}Bi_{0.25}Se_{0.896}$ (= $Sn_{0.582}Bi_{0.279}Se$).

Table S4: Coordinates, site occupancies and equivalent isotropic displacement parameters of rocksalt-type $Sn_{0.582}Bi_{0.279}Se$ in a sample with the nominal composition $Sn_5Bi_2Se_8$ = $Sn_{0.625}Bi_{0.25}Se$.

Atom	**Wyckoff position**	***x***	***y***	***z***	***s.o.f.* ***	**B_{iso} / $Å^2$**
Se1	4*a*	0	0	0	1	1.32(6)
Sn2/Bi2	4*b*	1/2	1/2	1/2	0.582 / 0.279	1.53(5)

* site occupancies constrained to composition $Sn_{0.582}Bi_{0.279}Se$.

Table S5: Crystallographic data and results of the Rietveld refinement of quenched $Sn_4Bi_2Se_7$ = $Sn_{0.57}Bi_{0.29}Se$ (x = 4, the composition was constrained to the nominal composition, which is not changed significantly by the small amount of SnSe as a side phase).*

formula	$Sn_{0.57}Bi_{0.29}Se_1$	SnSe
phase fraction	98 wt-%	2 wt-%
formula mass	206.54 $gmol^{-1}$	197.67 $gmol^{-1}$
crystal system	cubic	orthorhombic
space group	*Fm$\bar{3}$m*	*Pnma*
cell parameters	a = 5.95581(4)Å	a = 11.63(2) Å b = 4.196(7) Å c = 4.243(8) Å
cell volume	211.262(5) $Å^3$	207.0(6) $Å^3$
X-ray density	6.4935(2) gcm^{-3}	6.34(2) gcm^{-3}
Z	4	4
R_{Bragg}	0.009	0.008
radiation	Cu-$K_{\alpha1}$ (λ = 1.54051 Å)	
2θ range	4° < 2θ < 100°	
refined parameters	25	
background parameter	12	
R_p / R_{wp}	0.016 / 0.022	
GooF	0.955	

* For the rocksalt-type phases with x = 3 (see main text) and x = 4, microstrain peak broadening was considered by a Lorentzian function and crystallite-size broadening by a Gaussian function for $Sn_3Bi_2Se_6$ (x = 3) and a convolution of a Gaussian and a Lorentzian function for $Sn_4Bi_2Se_7$ and $Sn_5Bi_2Se_8$ (x = 4, x = 5), respectively. The peak broadening of SnSe due to crystallite size effects was described with a Gaussian function. Preferred orientation of SnSe was taken into account by spherical harmonics of the fourth order. The atomic parameters of SnSe were taken from literature [Adouby, K.; Pérez Vicente, C.; Jumas, J. C. *Z. Kristallogr.* **1998**, *213*, 343-349] and not refined, only the unit-cell parameters were refined.

Table S6: Coordinates, site occupancies and equivalent isotropic displacement parameters of rocksalt-type $Sn_4Bi_2Se_7$ = $Sn_{0.57}Bi_{0.29}Se$ (x = 4).

Atom	**Wyckoff position**	***x***	***y***	***z***	***s.o.f.***	**B_{iso} / $Å^2$**
Se1	4*a*	0	0	0	1	0.74(3)
Sn2/Bi2	4*b*	1/2	1/2	1/2	0.57 / 0.29*	1.03(2)

* s.o.f. constrained to match the nominal composition of $Sn_{0.57}Bi_{0.28}Se$.

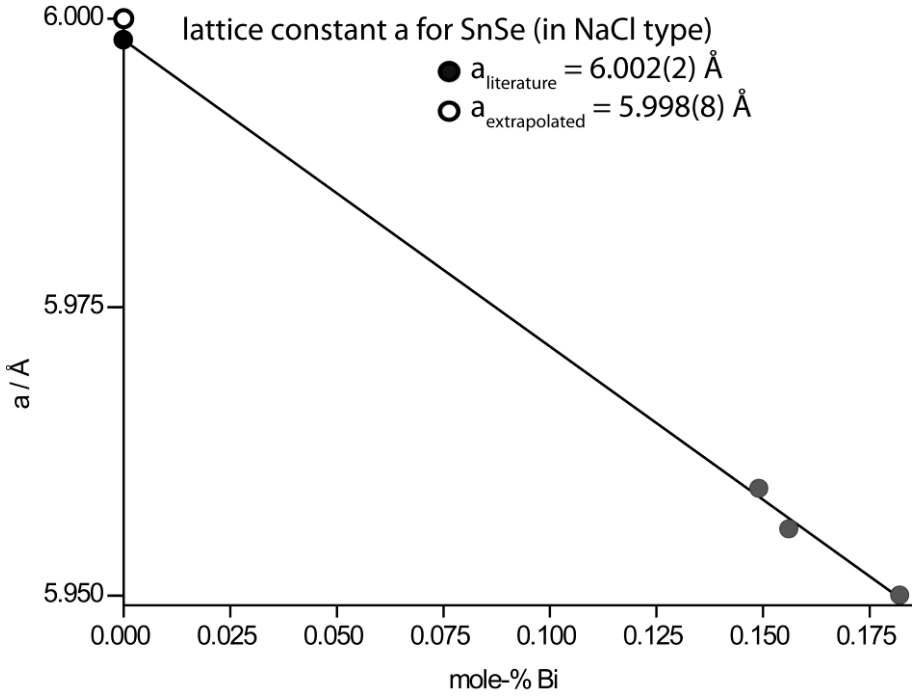

Figure S4: Lattice parameters of quenched rocksalt-type phases $(SnSe)_xBi_2Te_3$ (gray points) as a function of the Bi content (Vegard's law) with the extrapolated lattice parameter of SnSe in the NaCl structure type (black point) and the value reported for thin films of NaCl-type SnSe in the literature (empty circle; I. R. Nuriev, A. K. Sharifova, *Sov. Phys. Crystallogr.* **1989**, *34*, 635-636). The lattice parameters of the rocksalt-type phases decrease with increasing Bi_2Se_3 content, which can be explained by the simultaneously increasing number of vacancies and Bi^{3+} ions incorporated in the structure; Bi^{3+} ions are expected to be smaller than Sn^{2+} ions due to their higher charge. However, an explanation by means of the different ionic radii of Bi^{3+} and Sn^{2+} is not as straightforward as for other main group element ions because the ionic radius on Sn^{2+} is not determined reliably (cf. Shannon, R. D.; *Acta Crystallogr. Sect. A* **1976**, *32*, 751-767).

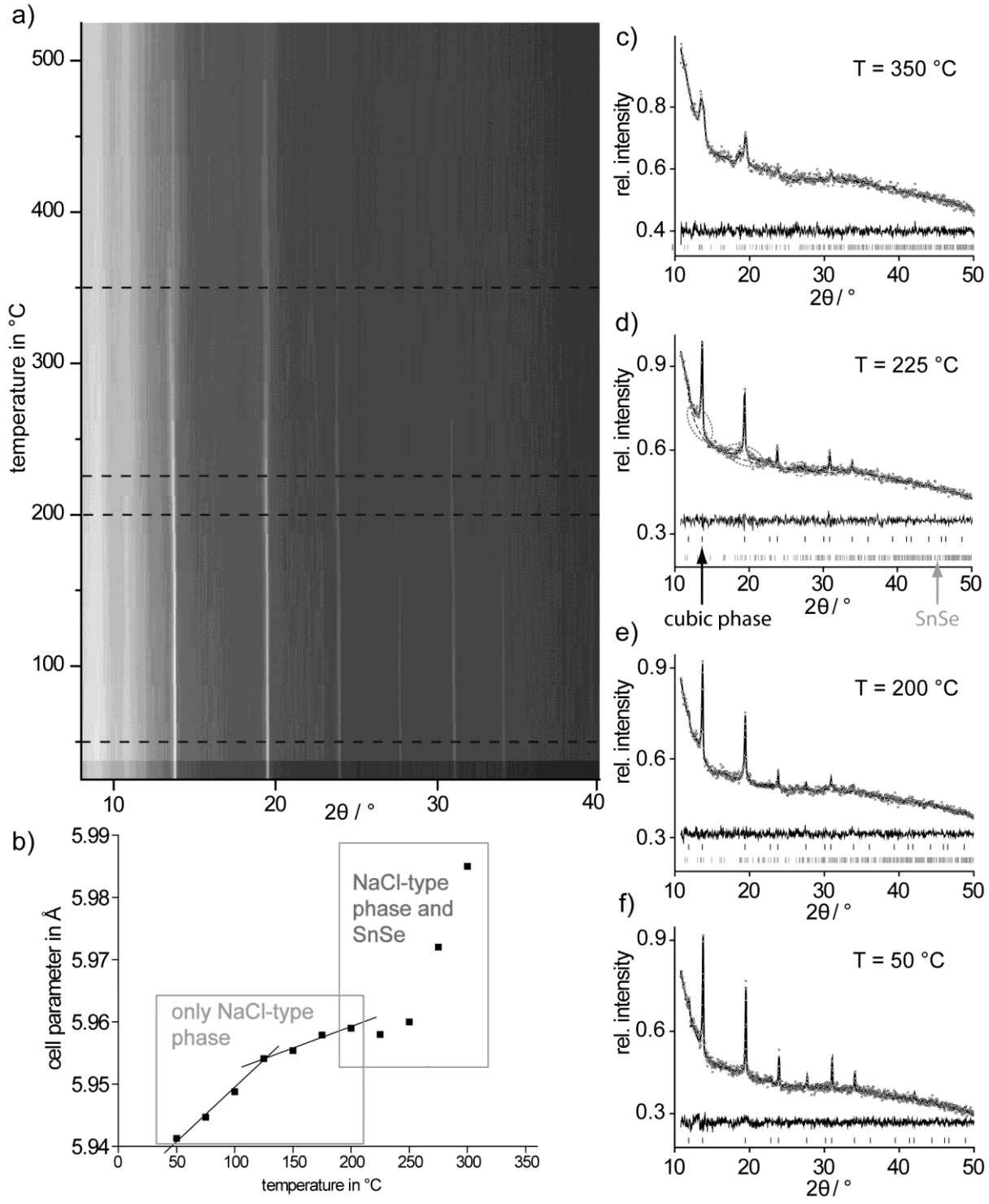

Figure S5: a) HT-PXRD plot for a quenched sample with the nominal composition $Sn_4Bi_2Se_7$ up to 500 °C, dotted lines indicate the patterns shown on the right [c)-f)]; b) progression of the cubic lattice parameter *a* upon heating with changing slope at 125 °C; c)-f) Rietveld refinements for selected patterns at different temperatures: data points are drawn as circles, calculated data as a black line, difference plot as a black line below, reflection positions indicated by vertical lines for the cubic phase (black) and for SnSe (gray); in d) dotted ellipsoids indicate misfits and the broken line represents the background fit.

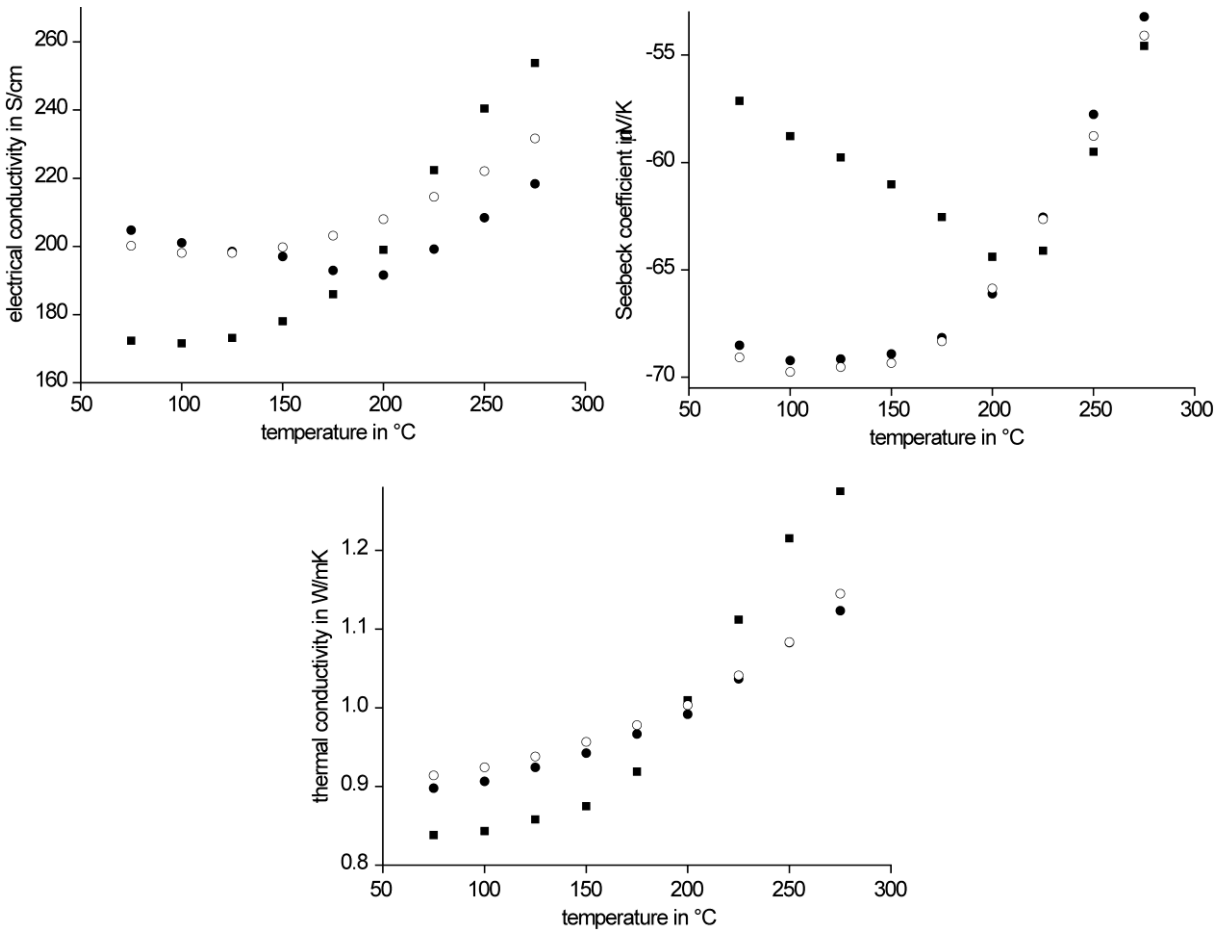

Figure S6: Thermal conductivity (bottom), Seebeck coefficient (top right) and electrical conductivity (top left) of a sample with the nominal composition $Sn_4Bi_2Se_7$ (black spheres = averaged heating curves and hollow spheres = averaged cooling curved after the decomposition, black squares = first heating step).

Difference Fourier maps:

The off-edge dataset of the L7,7-type structure was tested regarding a possible description as a twin in the lower symmetric space group *Cmc*2_1 instead of *Cmcm*. The following figures depict the residual electron densities around the interconnecting cation site between the NaCl-type slabs.

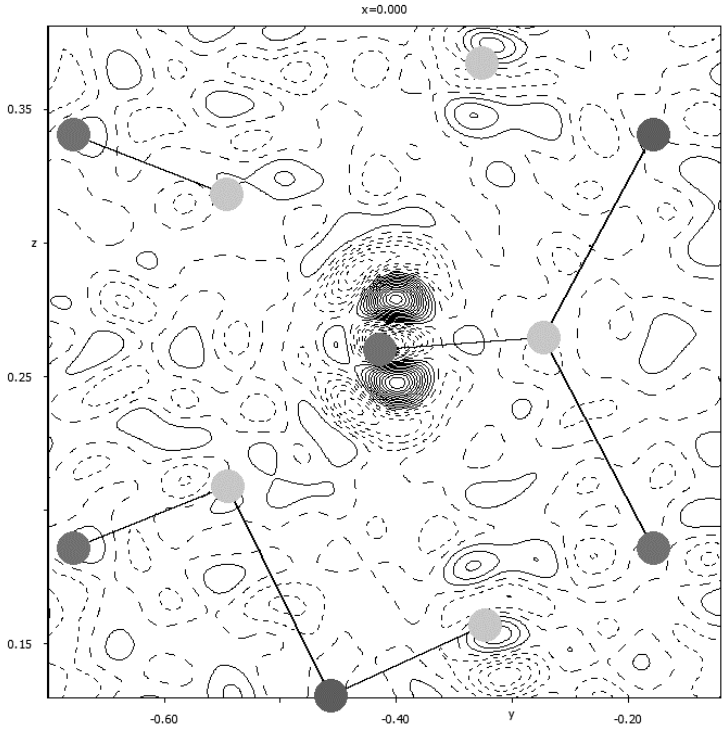

Figure S7: Residual electron densities around the cation site interconnecting the NaCl-type slabs for the structure refinement in space *Cmc*2_1 with a mirror plane perpendicular [001] as twin law; light gray circles depict Se atoms and dark gray circles depict the cation positions, contour = 0.5 electrons.

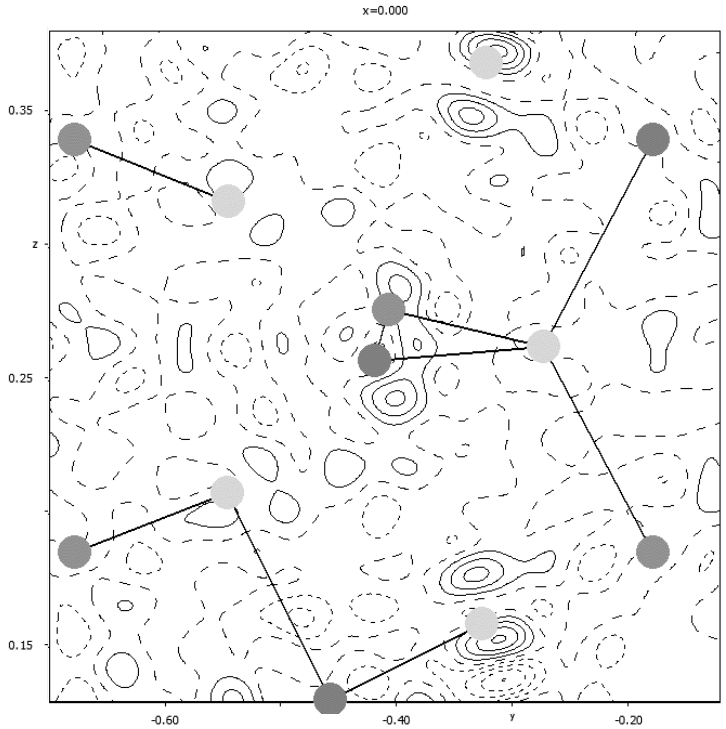

Figure S8: Residual electron densities around the cation site interconnecting the NaCl-type slabs for the structure refinement in space *Cmc*2_1 with split position for the interconnecting cation site. Light gray circles depict Se atoms and dark gray circles depict the cation positions, contour = 0.5 electrons.

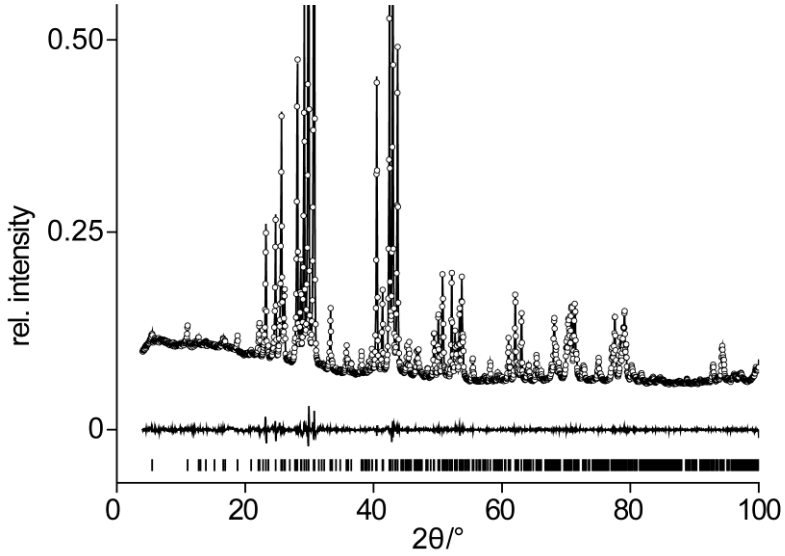

Figure S9: Rietveld refinement of a sample (annealed at 940 °C, then water-quenched) with the nominal composition $(SnSe)_2Bi_2Se_3$ (strongest reflection truncated at 55 % of max. intensity), data points drawn as circles, calculated data as black line; difference plot as black line below; reflection positions indicated by vertical lines; L7,7 model taken from the single crystal refinement of $Sn_{3.6}Bi_{3.6}Se_9$ (cf. Tables 5 and S7; cell parameters refined, atom coordinates fixed, refined overall isotropic displacement for anions and cations each); R_p = 0.021, R_{wp} = 0.027, GooF = 1.246 (preferred orientation taken into account by 6th order spherical harmonics with individual sets of parameters; crystallite size by convolution of a Gaussian and a Lorentzian function, microstrain by a Lorentzian function).

Table S7: Atom positions, site occupancies and equivalent isotropic displacement parameters (in Å^2) of $Sn_{3.6}Bi_{3.6}Se_9$ at RT, $U_{eq} = 1/3 \cdot [U_{11} + U_{22} + U_{33}]$.

Atom	Site	x	y	z	U_{eq}	s.o.f.	overall occupancy
Sn1 Bi1	8*d*	0	0.178251(19)	0.172730(9)	0.03128(10)	0.581(14) 0.376(7)	0.957(14)
Sn2 Bi2	8*d*	0	0.26869(2)	0.557211(11)	0.03052(13)	0.470(7) 0.291(4)	0.761(7)
Sn3 Bi3	8*d*	0	0.91382(5)	0.24109(3)	0.0496(4)	0.318(8) 0.149(4)	0.467(8)*
Sn4 Bi4	4*d*	0	0	0	0.03356(13)	0.379(11) 0.526(6)	0.905(11)
Sn5 Bi5	8*d*	0	0.456713(14)	0.117269(7)	0.03116(9)	0.241(7) 0.721(4)	0.962(7)
Se1	8*d*	0	0.09178(3)	0.083945(16)	0.02735(14)	1	1
Se2	8*d*	0	0.17557(4)	0.64464(2)	0.03905(18)	1	1
Se3	8*d*	0	0.36279(3)	0.027132(14)	0.02821(15)	1	1
Se4	8*d*	0	0.54594(3)	0.195491(17)	0.03029(14)	1	1
Se5	4*d*	0	0.27297(5)	0.25	0.0317(2)	1	1

* This site generates the split position between the NaCl-like slabs. The maximum occupancy is therefore limited to 0.5.

Table S8: Anisotropic displacement parameters (in Å²) of $Sn_{3.6}Bi_{3.6}Se_9$ at RT, defined as exp [$-2\pi^2 (U_{11}h^2 a^{*2} + U_{22}k^2b^{*2} + U_{33}l^2c^{*2} + U_{12}hka^*b^* + U_{13}hla^*c^* + U_{23}klb^*c^*)$].

Atom	U_{11}	U_{22}	U_{33}	U_{12}	U_{13}	U_{23}
Sn1 / Bi1	0.02925(17)	0.03174(17)	0.03284(19)	0	0	0.00018(10)
Sn2 / Bi2	0.0290(2)	0.0284(2)	0.0342(2)	0	0	-0.00116(13)
Sn3 / Bi3	0.0401(3)	0.0499(4)	0.0588(10)	0	0	0.0125(3)
Sn4 / Bi4	0.0330(2)	0.0343(2)	0.0334(2)	0	0	-0.00114(14)
Sn5 / Bi5	0.02860(15)	0.03082(15)	0.03406(16)	0	0	-0.00127(8)
Se1	0.0268(2)	0.0281(2)	0.0272(3)	0	0	0.00062(18)
Se2	0.0258(3)	0.0330(3)	0.0583(4)	0	0	-0.0144(2)
Se3	0.0269(3)	0.0271(2)	0.0306(3)	0	0	0.00115(19)
Se4	0.0305(2)	0.0317(2)	0.0287(3)	0	0	0.00046(17)
Se5	0.0336(3)	0.0323(3)	0.0291(4)	0	0	0

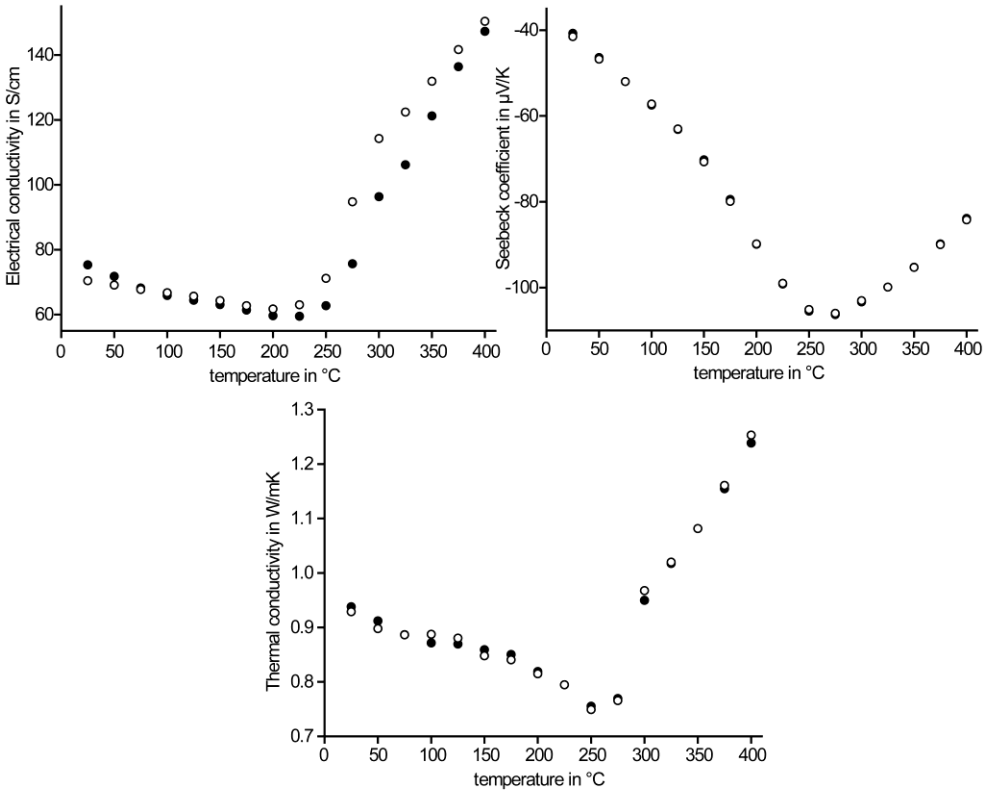

Figure S10: Thermoelectric characterization of $Sn_2Bi_2Se_5$ in the L4,4-lillianite type with full spheres for the averaged heating curved and empty spheres for the averaged cooling curved.

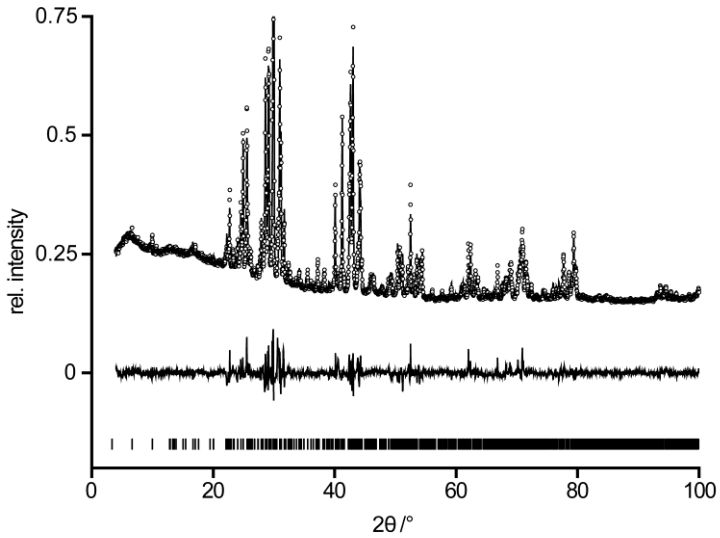

Figure S11: Rietveld refinement of a sample (annealed at 530 °C, then water-quenched) with the nominal composition $(SnSe)_{1.86}Bi_2Se_3$ (strongest reflection truncated at 75 % of max. intensity), data points drawn as circles, calculated data as black line; difference plot as black line below; reflection positions indicated by vertical lines; L4,7 model taken from the single crystal refinement of $Sn_{11.49}Bi_{12.39}Se_{30}$ (cf. Tables 6 and S9; cell parameters refined, atom coordinates fixed, refined overall isotropic displacement for anions and cations each); R_p = 0.024, R_{wp} = 0.038, GooF = 1.545 (preferred orientation taken into account by 8th order spherical harmonics with individual sets of parameters; crystallite size and microstrain by a Lorentzian function).

Table S9: Atom positions, site occupancies and equivalent isotropic displacement parameters (in Å^2) of $Sn_{11.49}Bi_{12.39}Se_{30}$ at RT; $U_{eq} = 1/3\ [U_{22} + 1/\sin^2\beta\cdot(U_{11} + U_{33} + 2U_{13}\cdot\cos\beta)]$.

Atom	Site	x	y	z	U_{eq}	s.o.f.	overall occupancy
Bi1 Sn1	4*d*	0.07005(2)	0.5	0.141175(10)	0.02552(9)	0.759(16) 0.21(3)	0.97(3)
Bi2 Sn2	4*d*	0.13068(2)	0.5	0.460970(10)	0.02280(9)	0.624(6) 0.330(10)	0.954(10)
Bi3 Sn3	2*d*	0	0	0	0.0300(2)	0.552(9) 0.35(2)	0.902(9)
Bi4 Sn4	4*d*	0.28113(3)	0	0.068288(16)	0.02496(14)	0.330(6) 0.407(10)	0.737(10)
Bi5 Sn5	4*d*	0.89381(2)	0	0.393771(12)	0.02533(10)	0.523(6) 0.404(10)	0.927(10)
Bi6 Sn6	4*d*	0.86202(3)	0	0.207953(13)	0.02516(11)	0.428(5) 0.495(10)	0.923(10)
Bi7a Sn7a	4*d*	0.14645(14)	0	0.31380(19)	0.0446(7)	0.078(7) 0.451(16)	1.01(2)
Bi7b Sn7b	4*d*	0.14368(13)	0	0.2890(2)	0.0487(9)	0.079(8) 0.400(16)	
Se8	4*d*	0.92760(4)	0	0.10109(2)	0.0197(2)	1	1
Se9	2*d*	0	0	0.5	0.0206(2)	1	1
Se10	4*d*	0.20920(5)	0	0.17447(3)	0.0336(2)	1	1
Se11	4*d*	0.25176(5)	0	0.42492(3)	0.0295(2)	1	1
Se12	4*d*	0.78336(5)	0	0.30005(2)	0.0264(2)	1	1
Se13	4*d*	0.02230(5)	0.5	0.36742(2)	0.02291(15)	1	1
Se14	4*d*	0.99936(5)	0.5	0.23563(2)	0.0229(2)	1	1
Se15	4*d*	0.14354(4)	0.5	0.03273(2)	0.0210(2)	1	1

Table S10: Anisotropic displacement parameters (in Å^2) of $Sn_{11.49}Bi_{12.39}Se_{30}$ at RT, defined as exp $[-2\pi^2 (U_{11}h^2 a^{*2} + U_{22}k^2b^{*2} + U_{33}l^2c^{*2} + U_{12}hka^*b^* + U_{13}hla^*c^* + U_{23}klb^*c^*)]$.

Atom	U_{11}	U_{22}	U_{33}	U_{12}	U_{13}	U_{23}
Bi1/Sn1	0.02592(16)	0.0223(2)	0.02880(15)	0	0.00495(10)	0
Bi2/Sn2	0.02132(16)	0.0203(2)	0.02692(15)	0	0.00291(10)	0
Bi3/Sn3	0.0323(3)	0.0277(3)	0.0304(3)	0	0.0052(2)	0
Bi4/Sn4	0.0227(3)	0.0228(2)	0.0293(2)	0	0.0024(2)	0
Bi5/Sn5	0.02404(18)	0.02265(17)	0.02960(17)	0	0.00422(12)	0
Bi6/Sn6	0.0245(2)	0.02238(18)	0.02848(18)	0	0.00201(13)	0
Bi7a/Sn7a	0.0468(7)	0.0384(6)	0.0498(17)	0	0.0101(7)	0
Bi7b/Sn7b	0.0487(8)	0.0353(7)	0.060(2)	0	-0.0036(8)	0
Se8	0.0198(3)	0.0188(3)	0.0201(2)	0	0.0008(2)	0
Se9	0.0230(4)	0.0192(3)	0.0203(3)	0	0.0052(3)	0
Se10	0.0232(3)	0.0176(3)	0.0570(4)	0	-0.0112(3)	0
Se11	0.0240(3)	0.0185(3)	0.0485(4)	0	0.0155(3)	0
Se12	0.0270(3)	0.0263(3)	0.0259(3)	0	0.0035(2)	0
Se13	0.0218(3)	0.0221(3)	0.0251(3)	0	0.0034(2)	0
Se14	0.0239(3)	0.0231(3)	0.0215(2)	0	0.0018(2)	0
Se15	0.0199(3)	0.0187(3)	0.0240(3)	0	0.0010(2)	0

Table S11: Atom positions, site occupancies and equivalent isotropic displacement parameters (in Å^2) of $Sn_{2.22}Bi_{2.52}Se_6$ at RT, $U_{eq} = 1/3 \cdot [U_{11} + U_{22} + U_{33}]$.

Atom	Site	x	y	z	U_{eq}	Occupancy	overall occupancy
Bi1 Sn1	2*d*	0.04893(4)	0.25	0.38866(8)	0.0222(2)	0.6555(6) 0.3445(6)	1.0 (constrained)
Bi2 Sn2	2*d*	0.13565(4)	0.75	0.16529(9)	0.0248(3)	0.5304(8) 0.4694(9)	0.9998(9)
Bi3 Sn3	2*d*	0.95145(4)	0.25	0.11162(8)	0.0224(3)	0.5567(6) 0.4433(6)	1.0 (constrained)
Bi4 Sn4	2*d*	0.13129(5)	0.25	0.66363(10)	0.0239(3)	0.4170(8) 0.4545(9)	0.8715(9)
Bi5a Sn5a	2*d*	0.2319(2)	0.25	0.9326(4)	0.0421(9)	0.2022(9) 0.2486(9)	0.8689(9)
Bi5b Sn5b	2*d*	0.2568(3)	0.25	0.9250(5)	0.058(2)	0.1601(9) 0.2580(9)	
Se6	2*d*	0.16865(9)	0.25	0.29901(17)	0.0253(5)	1	1
Se7	2*d*	0.00057(12)	0.75	0.2477(3)	0.0219(3)	1	1
Se8	2*d*	0.83461(9)	0.25	0.20255(16)	0.0238(5)	1	1
Se9	2*d*	0.09576(11)	0.25	0.0168(2)	0.0312(5)	1	1
Se10	2*d*	0.25193(11)	0.75	0.06892(10)	0.0285(3)	1	1
Se11	2*d*	0.09016(10)	0.75	0.51786(19)	0.0292(5)	1	1

Table S12: Anisotropic displacement parameters (in Å^2) of $Sn_{2.22}Bi_{2.52}Se_6$ at RT, defined as $\exp [-2\pi^2 (U_{11}h^2 a^{*2} + U_{22}k^2b^{*2} + U_{33}l^2c^{*2} + U_{12}hka^*b^* + U_{13}hla^*c^* + U_{23}klb^*c^*)]$.

Atom	U_{11}	U_{22}	U_{33}	U_{12}	U_{13}	U_{23}
Bi1/Sn1	0.0271(4)	0.0187(6)	0.0207(5)	0	0.0002(3)	0
Bi2/Sn2	0.0302(5)	0.0207(6)	0.0236(6)	0	-0.0012(4)	0
Bi3/Sn3	0.0260(4)	0.0186(6)	0.0226(5)	0	-0.0015(3)	0
Bi4/Sn4	0.0276(5)	0.0208(8)	0.0232(7)	0	-0.0004(4)	0
Bi5a/Sn5a	0.0437(15)	0.038(2)	0.0451(19)	0	0.011(2)	0
Bi5b/Sn5b	0.084(4)	0.036(2)	0.054(2)	0	0.027(4)	0
Se6	0.0244(8)	0.0244(14)	0.0271(13)	0	-0.0003(7)	0
Se7	0.0216(5)	0.0191(6)	0.0250(6)	0	-0.0036(4)	0
Se8	0.0252(8)	0.0227(13)	0.0234(12)	0	-0.0007(7)	0
Se9	0.0525(12)	0.0181(14)	0.0231(12)	0	-0.0091(9)	0
Se10	0.0292(6)	0.0279(7)	0.0285(6)	0	0.0038(11)	0
Se11	0.0442(11)	0.0194(14)	0.0239(11)	0	-0.0098(9)	0

Table S13: Atom positions, site occupancies and equivalent isotropic displacement parameters (in Å^2) of $Sn_{9.52}Bi_{10.96}Se_{26}$ at RT; $U_{eq} = 1/3\ [U_{22} + 1/\sin^2\beta\cdot(U_{11} + U_{33} + 2U_{13}\cdot\cos\beta)]$.

Atom	Site	x	y	z	U_{eq}	Occupancy	overall occupancy
Bi1 Sn1	2*d*	0.14995(4)	0	0.54479(3)	0.02237(16)	0.437(2) 0.563(2)	1.0 (constrained)
Bi2 Sn2	4*d*	0	0	0	0.0233(4)	0.144(12) 0.441(7)	0.585(12)
Bi3 Sn3	2*d*	0.49428(4)	0	0.16127(3)	0.0248(2)	0.430(6) 0.529(4)	0.959(6)
Bi4 Sn4	2*d*	0.75263(4)	0	0.08414(3)	0.0252(2)	0.050(6) 0.823(4)	0.873(6)
Bi5 Sn5	2*d*	0.55408(4)	0	0.37756(3)	0.02387(18)	0.565(2) 0.435(2)	1.0 (constrained)
Bi6a Sn6a	2*d*	0.2652(2)	0	0.2824(3)	0.0459(9)	0.623(7) 0.022(6)	0.996(7)
Bi6b Sn6b	2*d*	0.2517(4)	0	0.2560(3)	0.0415(12)	0.203(7) 0.148(6)	
Se7	2*d*	0.08739(9)	0	0.65320(6)	0.0237(3)	1	1
Se8a	2*d*	0.1222(15)	0	0.1171(11)	0.022(2)	0.59(10)	1.0 (constrained)
Se8b	2*d*	0.140(2)	0	0.133(2)	0.027(3)	0.41(10)	
Se9	2*d*	0.13055(9)	0	0.80592(6)	0.0234(3)	1	1
Se10	2*d*	0.21088(9)	0	0.41436(8)	0.0305(3)	1	1
Se11	2*d*	0.37515(8)	0	0.03943(5)	0.0204(2)	1	1
Se12	4*d*	0	0.5	0.5	0.0212(3)	1	1
Se13	2*d*	0.61927(9)	0	0.26934(6)	0.0256(3)	1	1

Table S14: Anisotropic displacement parameters (in Å^2) of $Sn_{9.52}Bi_{10.96}Se_{26}$ at RT, defined as exp $[-2\pi^2 (U_{11}h^2 a^{*2} + U_{22}k^2b^{*2} + U_{33}l^2c^{*2} + U_{12}hka^*b^* + U_{13}hla^*c^* + U_{23}klb^*c^*)]$.

Atom	U_{11}	U_{22}	U_{33}	U_{12}	U_{13}	U_{23}
Bi1/Sn1	0.0212(3)	0.0193(3)	0.0266(3)	0	0.0038(2)	0
Bi2/Sn2	0.0215(6)	0.0217(7)	0.0277(7)	0	0.0065(4)	0
Bi3/Sn3	0.0247(3)	0.0210(3)	0.0288(4)	0	0.0043(2)	0
Bi4/Sn4	0.0249(3)	0.0223(3)	0.0279(3)	0	0.0023(2)	0
Bi5/Sn5	0.0239(3)	0.0212(3)	0.0265(3)	0	0.0038(2)	0
Bi6a/Sn6a	0.0407(11)	0.0322(12)	0.061(2)	0	-0.0053(13)	0
Bi6b/Sn6b	0.0418(19)	0.0297(15)	0.056(3)	0	0.0165(19)	0
Se7	0.0236(5)	0.0225(6)	0.0246(6)	0	0.0020(4)	0
Se8a	0.021(3)	0.0176(14)	0.028(4)	0	0.009(3)	0
Se8b	0.024(4)	0.020(2)	0.037(8)	0	0.008(5)	0
Se9	0.0251(5)	0.0234(7)	0.0219(6)	0	0.0041(4)	0
Se10	0.0206(5)	0.0184(6)	0.0496(9)	0	-0.0040(5)	0
Se11	0.0212(5)	0.0188(6)	0.0215(6)	0	0.0044(4)	0
Se12	0.0224(7)	0.0191(8)	0.0211(8)	0	0.0003(6)	0
Se13	0.0266(6)	0.0258(7)	0.0242(6)	0	0.0036(5)	0

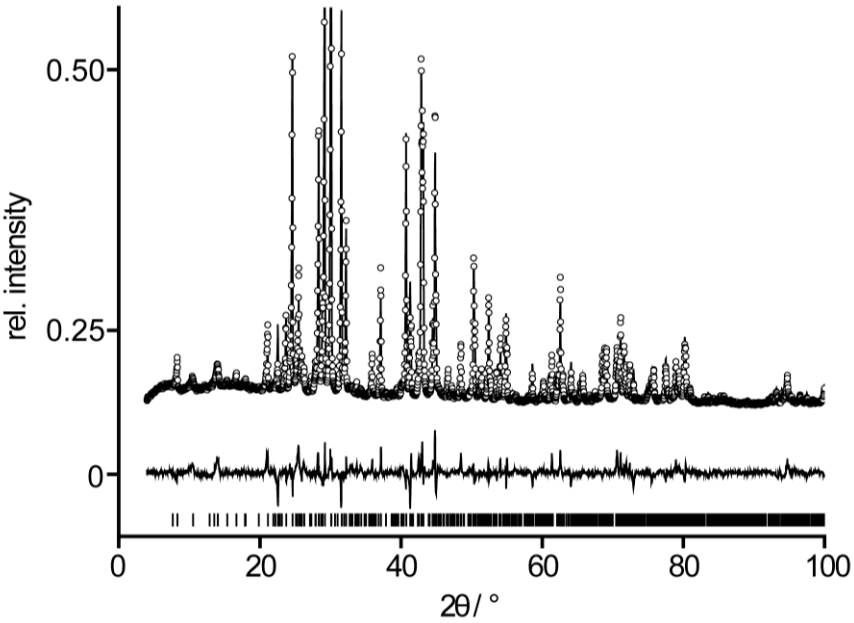

Figure S12: Rietveld refinement of a sample (annealed at 620 °C, then water-quenched) with the nominal composition $(SnSe)_2Bi_2Se_3$ (strongest reflection truncated at 55 % of max. intensity), data points drawn as circles, calculated data as black line; difference plot as black line below; reflection positions indicated by vertical lines; L4,4 model taken from the single crystal refinement of $Sn_{11.49}Bi_{12.39}Se_{30}$ (cf. Tables 7 and S11; cell parameters refined, atom coordinates fixed, refined overall isotropic displacement for anions and cations each); R_p = 0.027, R_{wp} = 0.042, GooF = 1.615 (preferred orientation taken into account by 6th order spherical harmonics with individual sets of parameters; crystallite size by a Lorentzian function and microstrain by convolution of a Gaussian and a Lorentzian function).

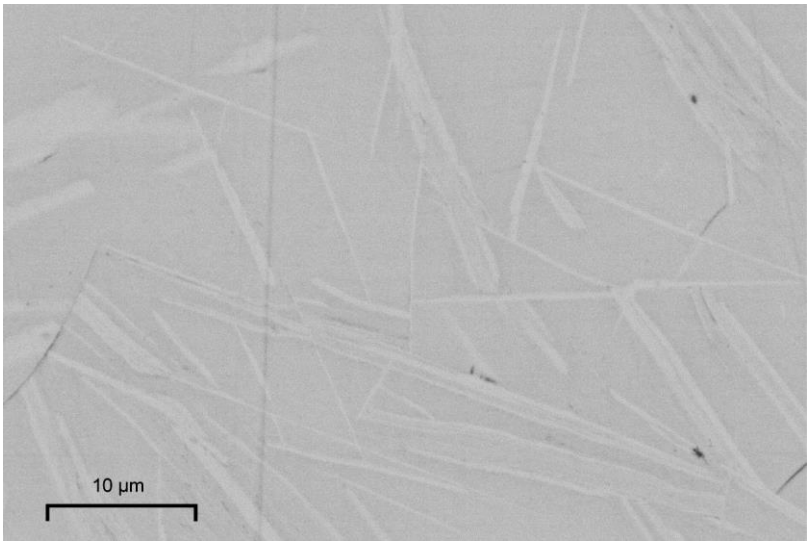

Figure S13: Backscattered electron SEM image of a sample with the nominal composition $Sn_2Bi_2Se_5$ after heating cycles of transport measurements with light gray areas showing the Bi-enriched phase (phase 1) and the dark gray areas showing the Sn-enriched phase (phase 2).

Table S15: Results of the chemical analyses of the sample (nominal composition: $Sn_2Bi_2Se_5$) shown in Fig. S13 (phase assignment according to Fig. S13).

	SEM-EDX	TEM-EDX
Phase 1 (bismuth-enriched)	$Sn_{16(1)}Bi_{28(1)}Se_{56(1)}$ (from 3 points)	$Sn_{15}Bi_{25}Se_{60}$
Phase 2 (tin-enriched)	$Sn_{23.6(8)}Bi_{22.8(7)}Se_{53.6(3)}$ (from 10 points)	$Sn_{22}Bi_{19}Se_{59}$

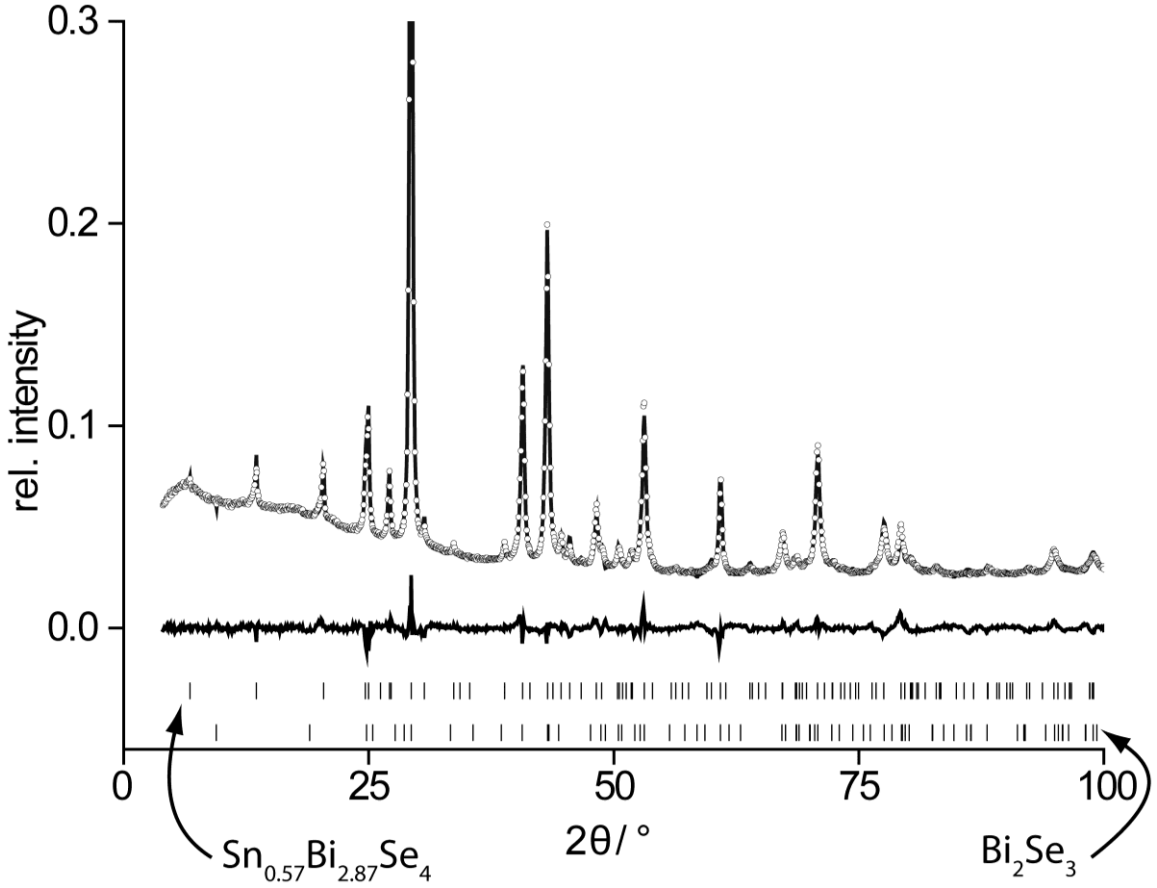

Figure S14: Rietveld refinement of sample with the nominal composition $(SnSe)_{0.5}Bi_2Se_3$ (annealed at 620 °C, then air-quenched); strongest reflection truncated at 30 % of max. intensity, data points drawn as circles, calculated data as black line; difference plot as black line below; reflection positions indicated by vertical lines for $Sn_{0.571}Bi_{2.286}Se_4$ (top row) and Bi_2Se_3 (bottom row).

Table S16: Results of the Rietveld refinement for a sample with the nominal composition (annealed at 620 °C, then air-quenched).

formula	$Sn_{0.584}Bi_{2.277}Se_4$	Bi_2Se_3
phase fraction	95 wt-%	5 wt-%
formula mass	2584.05 $gmol^{-1}$	654.84 $gmol^{-1}$
crystal system	trigonal	trigonal
space group	$R\bar{3}m$	$R\bar{3}m$
cell parameter	a = 4.1821(2) Å c = 39.178(4) Å	a = 4.1798(3) Å c = 28.026(5) Å
cell volume	593.42(8) Å³	424.0(1) Å³
Z	3	3
X-ray density	7.23 gcm^{-3}	7.69 gcm^{-3}
R_{Bragg}	0.015	0.044
radiation	Cu-$K_{\alpha1}$ (λ = 1.54051 Å)	
2θ range	4° < 2θ < 100°	
refined parameters	45 (thereof 24 for background)	
R_p / R_{wp} / GooF	0.024 / 0.034 / 1.616	

Tab. S17: Coordinates, site occupancies and equivalent isotropic displacement parameters of $Sn_{0.584}Bi_{2.277}Se_4$ and Bi_2Se_3 as obtained in the Rietveld refinement (cf. Figure S14 and Table S16).*

Atom	Wyckoff position	*x*	*y*	*z*	*s.o.f.*	B_{iso} / Å²
$Sn_{0.571}Bi_{2.286}Se_4$						
Se1	6*d*	1/3	2/3	0.5325(3)	1	1.1(1)
Se2	6*d*	1/3	2/3	0.3773(4)	1	1.1(1)
Bi1 Sn1	12*d*	1/3	2/3	2/3	0.443 *** 0.418 ***	1.1(1)
Bi2 Sn2	6*d*	1/3	2/3	0.2386(2)	0.917 *** 0.083 ***	1.1(1)
Bi_2Se_3						
Se1	6*c*	0	0	0.190(1)	1	1 **
Bi1	6*c*	0	0	0.391(5)	1	1 **
Se2	3*a*	0	0	0	1	1 **

* Peak broadening due to microstrain was taken into account by a Lorentzian function for $Sn_{0.571}Bi_{2.286}Se_4$ and a Gaussian function for Bi_2Se_3. Preferred orientation was taken into account by spherical harmonics of the eighth order for $Sn_{1.71}Bi_{6.86}Se_{12}$ and of the sixth order for Bi_2Se_3 with an individual set of parameters each.

** Displacement parameters were not refined as Bi_2Se_3 is a side phase with only ≈ 5 wt-%.

*** s.o.f.'s for $Sn_{0.584}Bi_{2.277}Se_4$ are derived from the results of the single crystal refinement of $Sn_{0.571}Bi_{2.286}Se_4$ according to the exsolution of Bi_2Se_3 based on the follwing reaction equation: $Sn_{0.571}Bi_{2.286}Se_4$ --> 0.95 $Sn_{0.584}Bi_{2.277}Se_4$ + 0.5 Bi_2Se_3. The alteration of the composition compared to $Sn_{0.571}Bi_{2.286}Se_4$ was assumed on position Bi1/Sn1.

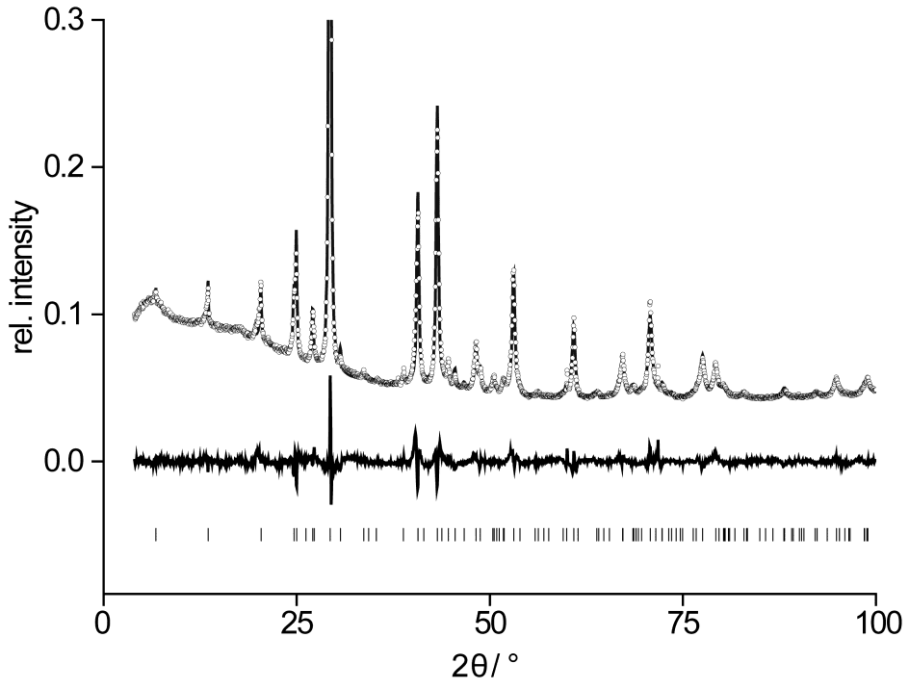

Figure S15: Rietveld refinement of the ~3 g sample (annealed at 500 °C for 9 d, then water-quenched) with the composition $SnBi_4Se_7$ = $(SnSe)_{0.5}Bi_2Se_3$ used for thermoelectric measurements (the strongest reflection truncated at 30 % of max. intensity): data points drawn as circles, calculated data as black line; difference plot as black line below; reflection positions indicated by vertical lines for $Sn_{0.571}Bi_{2.286}Se_4$ (top row) and Bi_2Se_3 (bottom row).

Table S18: Results of the Rietveld refinement of the ~3 g sample of $Sn_{0.571}Bi_{2.286}Se_4$ (annealed at 500 °C for 9 d, then water-quenched).

formula	$Sn_{0.571}Bi_{2.286}Se_4$
formula mass	2584.05 $gmol^{-1}$
crystal system	trigonal
space group	$R\bar{3}m$
lattice parameters *	a = 4.1831(2) Å c = 39.181(4) Å
cell volume	593.73(9) $Å^3$
X-ray density	7.23 gcm^{-3}
Z	3
radiation	Cu-$K_{\alpha1}$ (λ = 1.54051 Å)
2θ range	4° < 2θ < 100°
refined parameters	45, thereof 24 for background
R_p / R_{wp} / GooF	0.024 / 0.035 / 1.589
R_{Bragg}	0.012

* Deviations from the cell parameters determined for the single crystal may arise from different cooling rates.

Table S19: Coordinates, site occupancies and equivalent isotropic displacement parameters of annealed $Sn_{0.571}Bi_{2.286}Se_4$.

Atom	Wyckoff position	*x*	*y*	*z*	*s.o.f.* *	B_{iso} / $Å^2$
Se1	6*d*	1/3	2/3	0.5305(3)	1	0.74(9)
Se2	6*d*	1/3	2/3	0.3753(4)	1	0.74(9)
Bi1 Sn1	12*d*	1/3	2/3	2/3	0.452 0.405	0.74(9)
Bi2 Sn2	6*d*	1/3	2/3	0.2387(2)	0.917 0.083	0.74(9)

* s.o.f.'s taken from single crystal refinement.

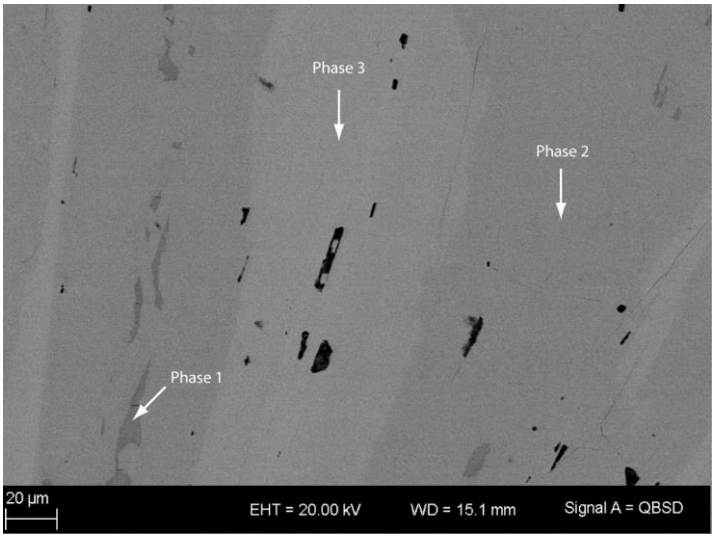

Figure S16: SEM-BSE image of a thermally treated sample (3 times cycled up to 500 °C) with the nominal composition $SnBi_4Se_7$. The image shows the presence of 2 majority and one minority phase after the thermal treatment during the thermoelectric measurements.

Table S20: SEM-EDX analyses for the sample with the nominal composition $SnBi_4Se_7$ after thermal treatment (3 times cycled up to 500 °C).

Element	nominal	Phase 1 (minority phase)	Phase 2 (majority phase)	Phase 3 (majority phase)
Sn / at-%	8.3%	21.9(6)	9.6(5)	5.6(5)
Bi / at-%	33.3%	24.3(4)	35.9(3)	39.9(4)
Se / at-%	58.3%	53.8(9)	54.5(10)	54.6(10)

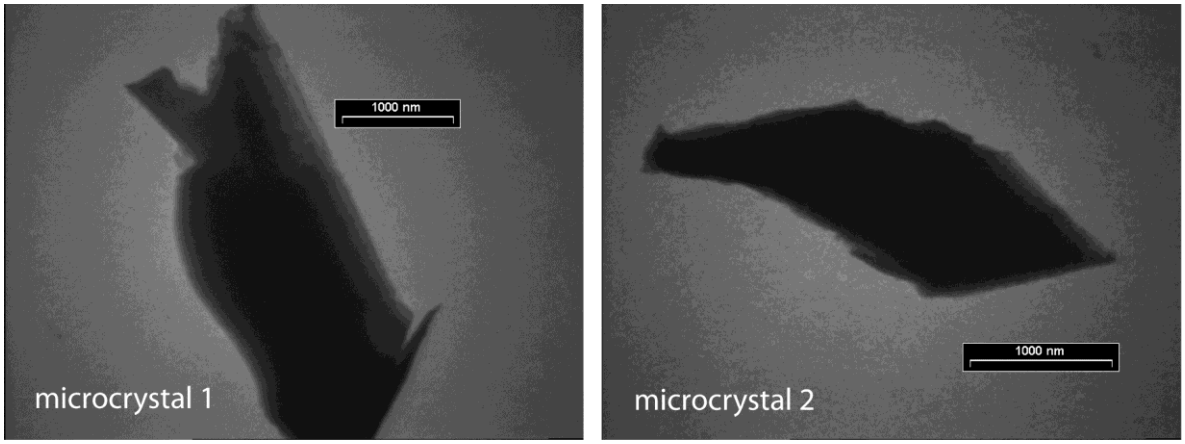

Figure S17: TEM images of two crystallites from a thermally treated sample (3 times cycled up to 500 °C) with the nominal composition $SnBi_4Se_7$.

Table S21: TEM-EDX analyses for the microcrystals from $SnBi_4Se_7$ after the thermal treatment (3 times cycled up to 500 °C).

Element	microcrystal 1	microcrystal 2
Sn / at-%	10.1(9)	7.1(8)
Bi / at-%	30.5(6)	34.5(8)
Se / at-%	59.3(9)	58.4(6)

Table S22: Crystallographic data and structure refinement of $Sn_{0.85}Bi_{2.15}Se_4$ (microcrystal 1 in Figure S17).*

formula	$Sn_{0.85}Bi_{2.15}Se_4$
formula mass	2597.3 $gmol^{-1}$
crystal system	trigonal
space group	$R\bar{3}m$
cell parameters	a = 4.1829(2) Å c = 39.158(3) Å
cell volume	593.34(6) $Å^3$
X-ray density	7.2689 gcm^{-3}
Z	3
absorption coefficient	8.096 mm^{-1}
F(000)	1071
radiation	synchrotron radiation (0.29470 Å)
2θ range	4.68° < 2θ < °26.2
absorption correction	semiempirical from equivalents (*SADABS* Version 2.05, Bruker AXS Inc., Madison, Wisconsin, USA, **2001**)
measured reflections	2282
independent data	254 [233 with $I > 2\sigma(I)$]
parameter	19
weighting scheme	$w = 1/[\sigma^2 F_o + 0.0001\, F^2]$
R1 / wR2 [$I > 2\sigma(I)$]	0.0278 / 0.0343
R1 / wR2 (all data)	0.0319 / 0.0371
GooF (all data)	1.54
$\Delta\rho_{min}$ / $\Delta\rho_{max}$	-1.37 $e Å^{-3}$/ 1.72 $e Å^{-3}$

* The initial refinement was based on the structure model described in Section 3.3.2 with Sn and Bi restricted to the same atom positions and displacement parameters when sharing one site. However, a refinement constrained to charge neutrality yielded occupancies of both cation positions of ~1 resulting in a rather Sn-rich sum formula ($Sn_{0.85}Bi_{2.15}Se_4$ = $Sn_{12.1}Bi_{30.7}Se_{57.1}$) as expected from EDX analysis (Table S21). Residual electron densities next to Se1 suggested using anharmonic displacement parameters up to the fourth order (Table S25). An explanation might be a reaction of the Se layer at the van der Waals gap to the additional Sn on the neighboring cation site, resulting in a slightly undulated Se layer.

Table S23: Coordinates, site occupancies and equivalent isotropic displacement parameters of $Sn_{0.75}Bi_{2.15}Se_4$; $U_{eq} = 1/3\ [U_{33} + 4/3(U_{11} + U_{22} – U_{12})]$.

Atom	Wyckoff position	*x*	*y*	*z*	*s.o.f.* *	U_{eq} / $Å^2$
Se1	4*b*	0	0	0.13537(13)	1	0.0235(11)
Se2	4*a*	0	0	0.28963(4)	1	0.0204(4)
Sn3 Bi3	3*d*	0	0	0	0.613 0.385	0.0252(3)
Sn4 Bi4	6*d*	0	0	0.42820(2)	0.120 0.881	0.0236(2)

* from harmonic SHELX refinement, e.s.d.'s ca. 0.002.

Table S24: Anisotropic displacement parameters of $Sn_{0.75}Bi_{2.15}Se_4$.

Atom	Wyckoff position	$U_{11} = U_{22}$	U_{33}	U_{12}	$U_{13} = U_{23}$
Se1	4*b*	0.142(10)	0.042(2)	0.0071(5)	0
Se2	4*a*	0.0210(5)	0.0192(7)	0.0105(2)	0
Sn3/Bi3	3*d*	0.0229(4)	0.0297(6)	0.0115(2)	0
Sn4/Bi4	6*d*	0.0216(3)	0.0278(4)	0.0108(2)	0

Table S25: Anharmonic displacement parameters site 4*b* (Se1) of $Sn_{0.75}Bi_{2.15}Se_4$.

C_{111}	C_{112}	C_{113}	C_{122}	C_{123}	C_{133}	C_{222}	C_{223}
-0.001(3)	-0.0006(14)	-0.0005(4)	0.0006(14)	-0.0002(2)	0	0.001(3)	-0.0005(4)
C_{233}	C_{333}						
0	**0.000116(16)**						
D_{1111}	D_{1112}	D_{1113}	D_{1122}	D_{1123}	D_{1133}	D_{1222}	D_{1223}
-0.041(12)	**-0.021(6)**	0.0003(4)	**-0.021(6)**	0.00014(19)	-0.00011(6)	-0.021(6)	-0.00014(19)
D_{1233}	D_{1333}	D_{2222}	D_{2223}	D_{2233}	D_{2333}	D_{3333}	
-0.00006(3)	0	**-0.041(12)**	-0.0003(4)	-0.00011(6)	0	-0.000001(3)	

Table S26: Comparison of the reported structures in the pseudo-binary system $SnSe\text{-}Bi_2Se_3$ with structure types, sum formulae and formulae normaized according to $(SnSe)_{\underline{x}}Bi_2Se_3$.

sum formula as used in the manuscript	structure type	sum formula according to $(SnSe)_x(Bi_2Se_3)$
$Sn_{0.582}Bi_{0.279}Se$*	NaCl-type	$(SnSe)_{4.17}(Bi_2Se_3)$, x ≈ 4.17
$Sn_{0.57}Bi_{0.29}Se$	NaCl-type	$(SnSe)_4(Bi_2Se_3)$, x = 4
$Sn_{0.5}Bi_{0.33}Se$	NaCl-type	$(SnSe)_3(Bi_2Se_3)$, x = 3
$Sn_{3.6}Bi_{3.6}Se_9$	L7,7-type	$(SnSe)_2(Bi_2Se_3)$, x = 2
$Sn_{11.49}Bi_{12.39}Se_{30}$	L4,7-type	$(SnSe)_{1.85}(Bi_2Se_3)$, x ≈ 1.85
$Sn_{2.22}Bi_{2.52}Se_6$	L4,4-type	$(SnSe)_{1.76}(Bi_2Se_3)$, x ≈ 1.76
$Sn_{9.52}Bi_{10.96}Se_{26}$	L4,5-type	$(SnSe)_{1.74}(Bi_2Se_3)$, x ≈ 1.74
$Sn_{0.85}Bi_{2.15}Se_4$**	$GeSb_2Te_4$-type	$(SnSe)_{0.79}(Bi_2Se_3)$, x ≈ 0.79
$Sn_{0.571}Bi_{2.286}Se_4$	$GeSb_2Te_4$-type	$(SnSe)_{0.5}(Bi_2Se_3)$, x = 0.5
$Sn_{4.11}Bi_{22.60}Se_{38}$***	its own structrue type	$(SnSe)_{0.36}(Bi_2Se_3)$, x ≈ 0.36

* nominal composition of the sample: $Sn_{0.625}Bi_{0.25}Se$

** decomposition product of $Sn_{0.571}Bi_{2.286}Se_4$, cf. Tables S22 to S25.

*** Structure is described in: Heinke, F.; Werwein, A.; Oeckler, O. Cation disorder and vacancies in the sulfosalt-like phase $Sn_{4.11}Bi_{22.60}Se_{38}$ - A resonant X-ray diffraction study. *J. Alloys Compd.* **2016**, *701*, 581-586.